

# EVALUATION OF THE SEISMIC RESPONSE OF FRAMES IMPLEMENTED WITH METAMATERIALS

Dina Hesham Mohamed Helmy<sup>1,2</sup>, Hesham El Arabaty<sup>3</sup>, Mohammed Nour<sup>4</sup>, Luca Placidi<sup>5</sup> and Mohammed Galal El Sherbiny<sup>6</sup>.

<sup>1</sup> Lecturer Assistant, Structural Engineering and construction management Department, Faculty of Engineering & Technology, Future University in Egypt (FUE). E-mail: dina.hesham@fue.edu.eg. Corresponding Author.

<sup>2</sup> Graduate researcher, Civil Engineering Department, Faculty of Engineering, Ain shams University, Egypt. E-mail:G19023551@eng.asu.edu.eg

<sup>3</sup> Professor of structural engineering, Structural Engineering Department, Faculty of Engineering, Ain shams University, Cairo, Egypt. E-mail: harabaty@yahoo.com.

<sup>4</sup> Professor of structural engineering, Structural Engineering Department, Faculty of Engineering, Ain shams University, Cairo, Egypt. E-mail: mnourf@yahoo.com.

<sup>5</sup> Associate Professor of Solid and Structural Mechanics, International Telematic University Uninettuno, C.so Vittorio Emanuele II, 39, 00186 Roma, Italy. E-mail: luca.placidi@uninettunouniversity.net.

<sup>6</sup> Associate Professor of Structural Engineering, Faculty of Engineering & Technology, Future University in Egypt (FUE). E-mail: m.galal@fue.edu.eg, mgkhleel@yahoo.com.

## ABSTRACT

This research aims at introducing a new idea in the design of frames to eliminate or suppress the transmission of waves through the structure in a certain designated range of frequencies that is called hereinafter as frequency band gap. To achieve this goal, we apply a concept from the mechanics of metamaterials to the investigated structural system by proposing a new beam-column connection in a multistory 2D frame. Modal and harmonic analysis are carried out for both the new proposed frame and the ordinary one in order to investigate the response of both systems. A thorough time history analysis is applied, also we demonstrate the response of the new proposed model under the loading of 9 different earthquake loads and a comparison between the resulted displacement and base shear is performed. Furthermore, a realization of the new connection is demonstrated. Results, comparison, and discussion are presented. The results show that the new proposed frame exhibits the calculated frequency band gap and the effect of seismic waves with frequencies within the bandgap frequency range was significantly mitigated. The novelty of this research is the ability of the new proposed idea to generate and tailor a frequency band gap in order to prevent the transmission of waves in this range of frequencies through the structural system itself. Consequently, the bandgap range of frequencies for each structure can be tuned depending on the seismic risk of its region on the global scale. This new feature could have a great impact and significant application to mitigate the effects of seismic waves on a structure.

Keywords: Frequency band gap, Metamaterials, Vibration, Waves, Modal analysis, Harmonic analysis, Frames, Beam-column connection, Time-history analysis.

## 1. Introduction

Metamaterials can be considered as engineered materials; they are made of a group of any kind of elements that are organized in repeating patterns. The geometry of the metamaterial structure [1][2] can make it cloak elastic waves for a specific range of frequencies. Thus, metamaterials [3][4][5] can protect structures from vibration [6][7][8]. That specific range of frequencies is called bandgap [9][10][11] and it is related to a unique elastic coefficient called cosserat couple modulus as proved by Madeo et al. [12].

In 2018, El-Sherbiny et al. [13] have analyzed the response of three different 1D continuum models under the effect of harmonic load excitation. The models exhibited a highly attenuated response in a range of frequencies that is called the band gap frequency. Also, they presented the analytical expressions of the upper and lower limits of such a band gap. Moreover, they numerically analyzed a 2D geometry with uniformly distributed oscillators to investigate its response under longitudinal or transverse excitation. Under harmonic load excitation and using FE program simulations, the model was analyzed, and the resulted band gap was calculated.

Furthermore, in [14] a 3D printed microstructure is experimentally tested. It contains a density of resonators using a shaking table device and a frequency bandgap was obtained as expected.

Also, dell'Isola F et al. [15] performed numerical simulations on a pantographic 2D lattice in order to find suitable

inclusions that can damp selected frequencies.

This paper demonstrates and discusses the harmonic analysis of a 2D reinforced concrete frame. Since the study of waves is indirectly the study of a simple harmonic motion, we can discuss the work of many researchers who presented time-history analysis for seismic metamaterial structures and the effect of the metamaterial concept on the propagation of waves.

Firstly, Brûlé et al. [16] demonstrated an experiment about a seismic metamaterial consisting of a mesh of vertical empty inclusions bored in the initial soil. The metamaterial structure was exposed to seismic waves generated by a monochromatic vibro-compaction probe. The energy in the field was measured before and after installing the boreholes and a strong reflection of surface waves by the seismic metamaterial has been confirmed.

In 2016, Colombi et al. [17] studied a meta-surface made of spatially graded subwavelength resonators on an elastic substrate. They concluded that this seismic metamaterial structure can convert the destructive seismic waves into harmless bulk shear waves when the waves have been approaching the short side of the wedge. Moreover, when approaching the long side of the wedge, the waves have been diverted into the bulk.

Moreover, an elastic metamaterial with periodically square concrete filled steel piles embedded in soil was analyzed by Du et al. [18]. They achieved a seismic shield for guided Lamb waves and surface waves. Complete band gap with specific frequencies were developed. They found that the periodic composite consisting of periodic square shaped piles produces a wider band gap than that of rectangular or cylindrical shaped piles. Band gap highly depends on the shape, dimensions, and material properties of the structure.

A new design paradigm of composite foundations was proposed by Casablanca et al. [19]. It retains the resistance of a standard foundation to a vertical load (i.e., a building on top), while offering the advantage of filtering the energy of S-waves propagating through it with frequencies within its band gap.

It was concluded that S-waves with frequencies greater than 4.5 Hz (the starting frequency of the theoretical band gap) are attenuated and that the device studied can filter more than 50% of the wave energy within that band gap.

In 2021, Palermo et al. [20] investigated the propagation of waves in a non-linear metasurface consisting of an array of non-linear oscillators attached to the free surface of a homogenous substrate. Then, they studied the influence of non-linearity on the spectral gap width and frequencies. Moreover, they investigated the combined effects of non-linearity and energy loss on the dispersive properties of the metasurface.

In addition, Dian-Kai Guo et al. [21] explored the coupled interference of the seismic resonators with the anisotropy of the surrounded soil material so that the seismic waves, within a certain frequency range, can be cancelled for earthquake protection.

Furthermore, Xiao Wang et al. [22] proposed 1D and 2D seismic metamaterials composed of common building materials to avoid expensive materials. The seismic metamaterial consisting of periodic infilled pipes filtered the Rayleigh waves and the band gap width depended on the distance between two adjacent infilled pipes and the properties of the soft filling material.

Xinyue Wu et al. [23] succeeded to broaden the band gap in a low frequency range by proposing a seismic metamaterial structure consisting of pillars above the ground and core-shell inclusions embedded in the soil. This metamaterial structure is aimed for protecting large infrastructures or civil engineering architectures.

A novel type of 2D seismic metamaterial was demonstrated by Ting Ting Huang et al. [24]. The metamaterial structure consisting of auxetic foam-coated hollow steel columns was analyzed and a parametric study was performed. The width of the band gap depended on the shape and height of the unit cell in addition to the properties of the auxetic foam.

The geometry and material of the seismic metamaterial structure play a major role in cloaking seismic waves and controlling the width of the band gap as presented by T. Venkatesh Varma [25]. They studied several seismic metamaterials with different geometries and materials and consequently they found that the steel columns are more effective but expensive. Non-reinforced concrete could be a more effective alternative when casted as columns coated with soft soil. Also, Xingbo Pu et al. [26] controlled the surface waves artificially using periodic wave barriers.

Lei Xiao et al. [27] explored that the soil-structure interaction can improve the seismic mitigation performance of a periodic foundation. Likewise, Xinnan Liu et al. [28] introduced a combined layered periodic foundations with different unit cells in tandem as seismic metamaterial structure. They also studied varying configurations of the metamaterial and showed its low starting frequency attenuation zones.

The application of metamaterials is also introduced in railways by Ting Li et al. [29] to shield the ground vibrations resulted from the high-speed rail system. They developed a 3D coupled train-track-soil interaction model and investigated the variation of the number of inclusions, the distances, and the train speeds on the mitigation effects for the induced ground vibrations.

Xingbo Pu et al. [30] proved the importance of fluid-solid interaction in the dynamics of the seismic metasurfaces. They analytically studied the seismic metasurfaces while propagating Rayleigh waves through a porous layer of soil equipped with

local resonators and showed that the band gap is influenced by the variation of the water table level. Also, Wenlong Liu et al. [31] proposed an ultra-wide band gap metasurface and applied it in bridge engineering.

Colombi A et al. [32] discussed in detail the role of the metabarrier and the metafoundation in the mitigation of seismic waves impact on buildings. The metabarrier surrounds the structure and cloaks the seismic waves and the metafoundation supports the structure and reduces the effect of waves. They performed a full 3D numerical simulation considering various parameters such as soil type, size, number of resonators and source directivity.

Jean-Jacques Marigo et al. [33] simulated an array of plates over a semi-infinite elastic ground and analyzed its effect on the propagation of the seismic waves. Also, periodically arranged built up steel section in a soil medium showed a 50% reduction in surface wave amplitude as presented by Muhammad et al. [34].

Meng Wang et al. [35] introduced a negative stiffness amplifying damper [36] that provides approximately 20% increase in the energy dissipation for long period structures.

So, metamaterials can be useful in vibration isolation and acoustics for their ability in filtering elastic waves. Band gap width and frequency depend on the geometry and material properties of the system. The metamaterial system can be installed in the soil surrounding the host structure or in the foundations of the structure or in the structural system itself as we introduce in our research. The inclusion of metamaterial concept in the structure will be introduced and discussed in section 2, then the development of the proposed model will be presented in section 3 and at last the results of the harmonic analysis and time-history analysis applied on both ordinary and new model will be presented in section 4.

## 2. The innovative idea

All previous researches discussed in sec.1 demonstrated the application of the concept of metamaterials either by using metamaterial structures installed in the soil surrounding the host structure or in the foundations of the structure or by installing external devices in the structure such as tuned-mass dampers.

The novelty of this research is to build a structure that acts like a metamaterial itself and to apply the concept of metamaterials in the structural building system. For a simple 2D frame, this idea can be achieved by converting the perfect rigid beam-column connection to an elastic one as shown in Fig.1. In other words, we introduce a connection in which the girder is connected to the column vertically through a roller support rested on a bracket connected to the column and horizontally by a spring, see Fig.1(c). This new form of connection in all beam-column joints of the frame and the repeating pattern of the spring mass system at each storey along the whole structure give the frame new features. When the structure is exposed to incoming waves, the springs will oscillate and cancel the effect of incoming waves at a certain tuned range of frequencies that is called herein a bandgap [37] and it is the most important feature in this research. This feature ensures that no waves in the range of frequency band gap can be transmitted through the structure. The band gap limits are  $\omega_1$  and  $\omega_2$  or the range of frequencies of the band gap can be determined by the equations (1) and (2) presented by El-Sherbiny et al.[13].

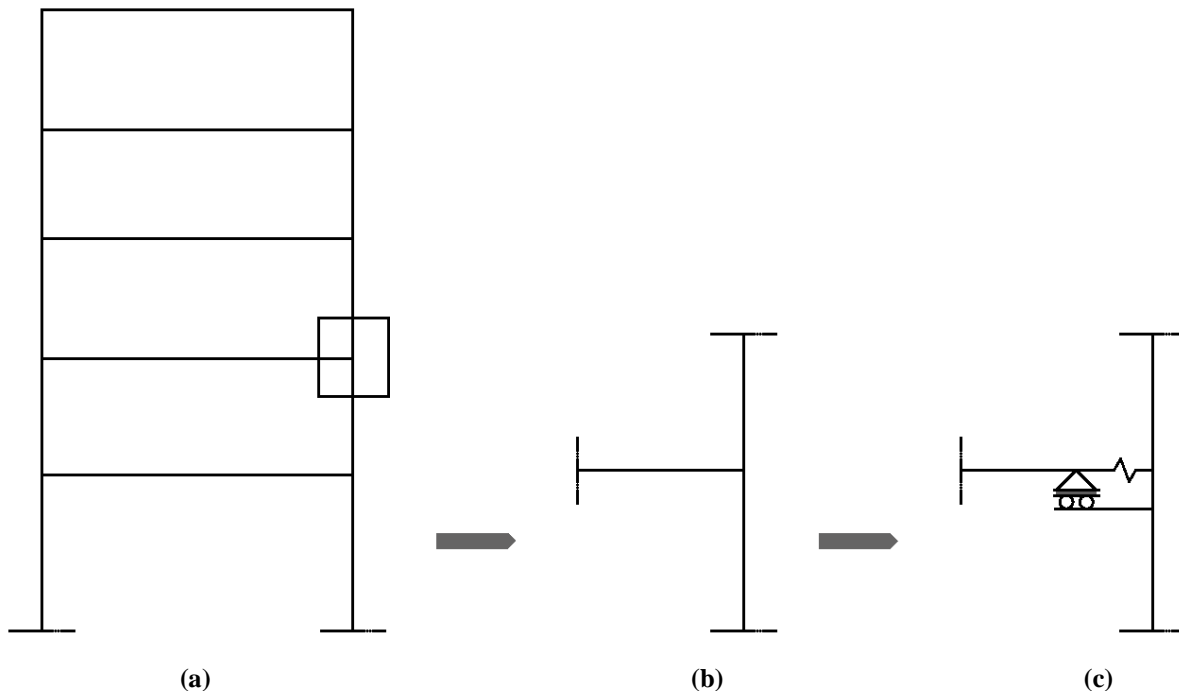


Fig. 1 The difference between the ordinary rigid connection and the proposed connection. a) Typical 2D frame, b) Typical beam-column joint, c) The new proposed connection.

$$\omega_1 = \sqrt{\frac{k}{m}} \quad (1) \quad , \quad \omega_2 = \sqrt{\frac{k}{\rho} + \frac{k}{m}} \quad (2)$$

Where  $\omega_1$  is the first band gap limit, and  $\omega_2$  is the second band gap limit,  $k$  is the stiffness of springs per unit length,  $m$  is the resonators mass per unit length and  $\rho$  is the host mass per unit length. These parameters will be discussed in detail in the next section.

In order to visualize this connection in real life, it can be a laminated rubber bearing with tailored stiffness depending on the tuned bandgap. Zhang et al. [38] studied the hysteretic behavior of a laminated rubber bearing under displacement loading, see Fig.2, and deduced its stiffness that can be tailored upon the specimen's geometry characteristics. For the proposed connection in this research, we can tailor a laminated rubber bearing with the needed stiffness value in order to obtain the required range of frequency bandgap.



Fig. 2 Laminated rubber bearing specimen under displacement loading.

### 3. Proposed Model and Analytical Technique

In order to investigate the idea explicated in section 2, we illustrate it with an example. Thus, we propose a 2D reinforced concrete frame consisting of 10 stories as shown in Fig. 3. The simulation is realized through ANSYS where all beam-column constraints have the new proposed connection illustrated in Fig.1c. The typical girder with a mass  $m_b$  has a periodic arrangement and it is modelled as a concentrated mass connected laterally to columns having a typical height  $H$  by a double spring one on the left and the other is on the right-hand side of the girder. The girder is simulated as a structural mass element on one node in the middle of the storey, the connection between the structural mass element and the column is modelled as a spring-damper combination element. The reinforced concrete columns are clamped at the base and the physical properties of the model are given in table 1.

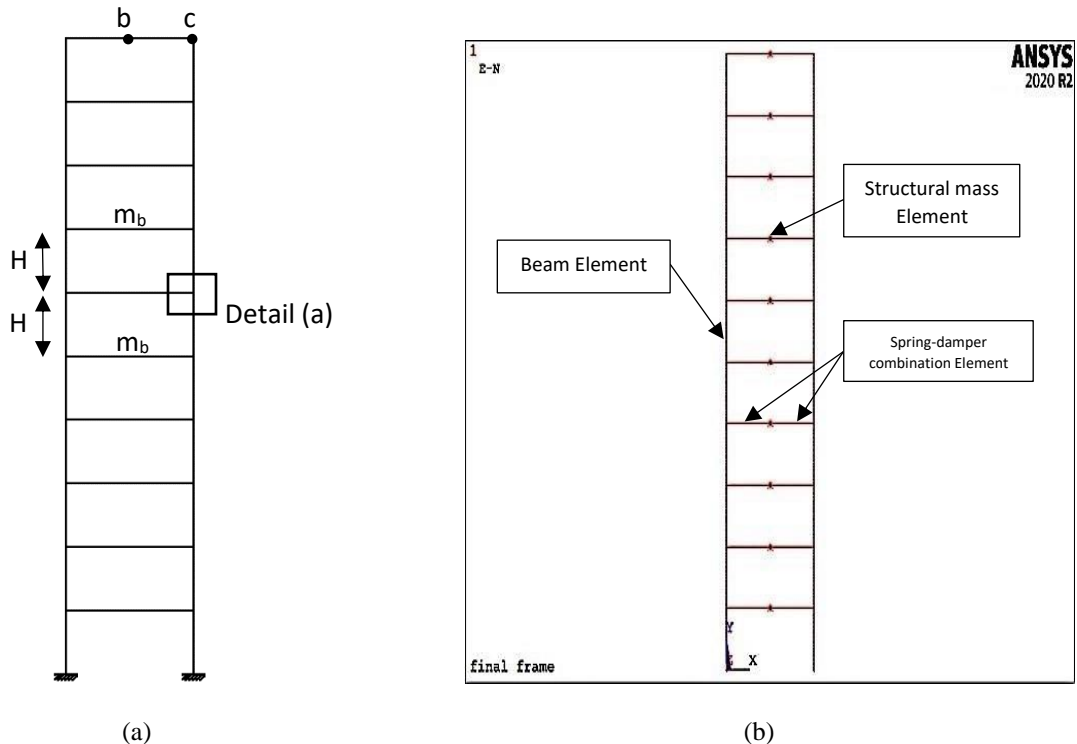


Fig. 3 a) The proposed frame, detail (a) is the proposed connection from Fig.1, b) The frame model on ANSYS 2020 with detailed elements.

The proposed model is shown in Fig. 3, where a girder having a mass  $m_b$  is connected laterally to a column having a constant cross section area through a spring of stiffness  $k_s$ . The band gap limits of this model are determined using Eq. 1,2 and the parameters of these equations corresponding to the physical properties introduced in table 1 are presented in Eq. 3, 4 and 5.

$$k = \frac{2k_s}{H} \tag{3}$$

$$m = \frac{m_b}{H} \tag{4}$$

$$\rho = 2A * \gamma \tag{5}$$

Where  $k_s$  is the stiffness of the spring,  $H$  is the typical story height,  $m_b$  is the mass of the girder,  $A$  is the cross-section area of the column and  $\gamma$  is the density of the concrete that was modelled as a linear isotropic material with a  $2E+10 \text{ kg/m}^2$  young's modulus and a 0.3 Poisson's ratio.

Table 1. The properties of the frame analyzed by the FE program.

Parameter	Value	Parameter	Value
$k_s$ (N/m)	4935000	$K$ (N/m <sup>2</sup> )	$3.29 \times 10^6$
$m_b$ (Kg)(in X-direction)	10000	$m$ (kg/m)	3.33
$H$ (m)	3	$\rho$ (kg/m)	800
$A$ (m <sup>2</sup> )	0.4 x 0.4	$\omega_1$ (rad/s)	31.4
$\gamma$ (kg/m <sup>3</sup> )	2500	$\omega_2$ (rad/s)	71.4

and the band gap limits values are;

$$f_1 = \frac{\omega_1}{2\pi} = 5 \text{ Hz}, f_2 = \frac{\omega_2}{2\pi} = 11.36 \text{ Hz} \tag{6}$$

Thus, as a matter of facts, for the proposed model and the given physical properties, the band gap limits are obtained (Eq.6) and the frequencies in the range between  $f_1 = 5 \text{ Hz}$  and  $f_2 = 11.36 \text{ Hz}$  will be eliminated under harmonic loading.

A comparison will be performed in the next section between the proposed frame consisting of typical double spring system and an ordinary concrete frame through modal, harmonic analysis, and time-history analysis.

#### 4. Results and discussion

##### 4.1 Modal Analysis Results and Discussion

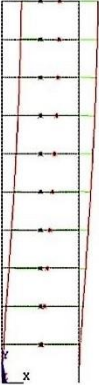
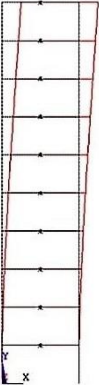

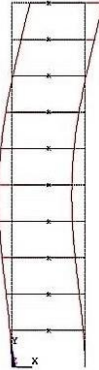
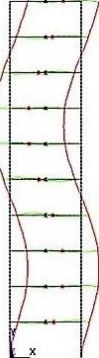
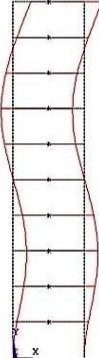

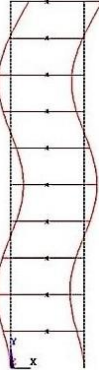
A modal analysis was conducted for two models using the FE program ANSYS. The first model is an ordinary frame with a column-frame connection of the type of Fig. 1b and the second one is a frame with the same physical properties but with a frame-column connection of the type of Fig. 1c. The modal analysis results of the ordinary frame compared to the proposed frame are presented in Table 2.

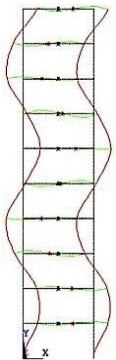

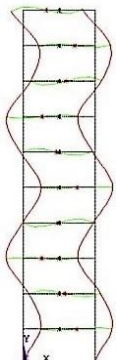
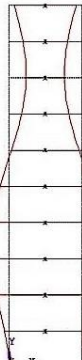
Table 2. Comparison of frequencies (Hz) modal analysis results between the ordinary frame and the proposed frame.

Mo- de no.	Ordinary Frame	Proposed Frame
1	0.608	0.203
2	1.89	1.27
3	3.4	3.55
4	5.096	6.96
5	7.04	10.21
6	9.217	10.525
7	11.532	11.4892
8	13.813	11.528
9	15.8017	13.4719
10	17.1753	16.4964

The difference between the mode shapes of the two models is shown in Table 3.

Table 3. Comparison of mode shapes for the ordinary frame and the proposed frame.

Mode no.	Ordinary Frame	Proposed Frame
1	$f_1 = 0.61 \text{ Hz}$ 	$f_1 = 0.203 \text{ Hz}$ 
2	$f_2 = 1.89 \text{ Hz}$ 	$f_2 = 1.27 \text{ Hz}$ 
3	$f_3 = 3.4 \text{ Hz}$ 	$f_3 = 3.55 \text{ Hz}$ 
4	$f_4 = 5.09 \text{ Hz}$ 	$f_4 = 6.96 \text{ Hz}$ 

5	$f_5 = 7.05 \text{ Hz}$ 	$f_5 = 10.2 \text{ Hz}$ 
6	$f_6 = 9.2 \text{ Hz}$ 	$f_6 = 10.5 \text{ Hz}$ 

The above results show:

- The fundamental frequency of the proposed frame is lower than that of the ordinary one, and this can be explained with a reduction of the stiffness in the joint and therefore in the whole system.
- In Table 3, the fifth and sixth mode fall in the frequency band gap. Thus, the corresponding mode shapes of first and second columns are considerably different.
- The mode shapes of the proposed frame varied more noticeably than that of the ordinary frame, also the top relative displacement diminished remarkably in the 5<sup>th</sup> and 6<sup>th</sup> modes as shown in rows 5 and 6 in table 3.

#### 4.2 Harmonic Analysis Results and Discussion

Both models have been analyzed under horizontal harmonic excitation (Eq. 7) at the base of the frame. The excitation frequency ranges from 0 to 15 Hz. Damping is not introduced in the analysis.

$$y_s(t) = y_o \sin \omega t \quad (7)$$

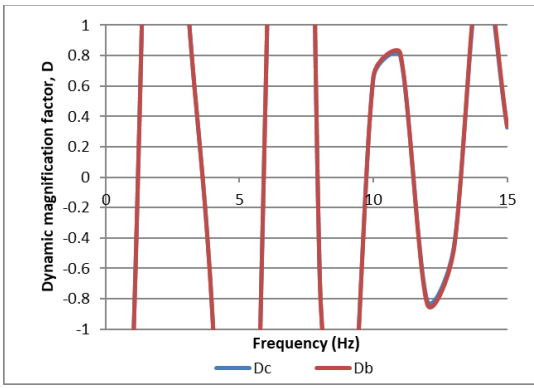
Where  $y_s(t)$  is the imposed support displacement at the basis,  $y_o$  is the excitation amplitude of the imposed displacement set to 1 mm,  $\omega$  is the excitation angular frequency and  $t$  is the time.

The response of both frames are reported in Fig.4, in terms of the dynamic magnification factor  $D(= y_i/y_o)$  as a function of the excitation frequency  $f = \omega/2\pi$ , where  $y_i$  is the amplitude of the displacement response related to a general point,  $y_{tb}$  is the amplitude of the displacement at the top of the frame in the middle of the beam in the steady-state response (see point b in fig.3) and  $y_{tc}$  is the amplitude of the displacement at the top of the frame in the column in the steady-state response (see point c in fig.3).

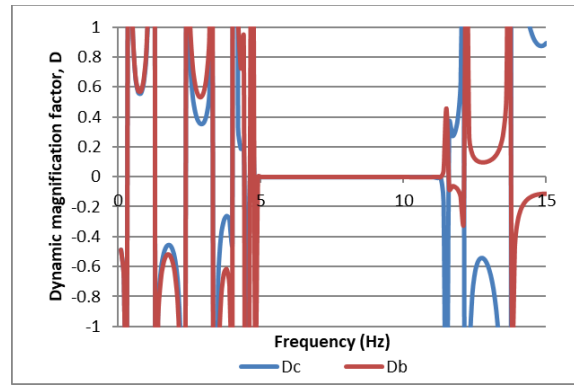
The magnification factors that are visualized in Fig.4 are defined as follows,

$$D_b = y_{tb}/y_o \quad (8)$$

$$D_c = y_{tc}/y_o \quad (9)$$



(a)



(b)

Fig. 4 Harmonic analysis results (a) the response of the ordinary frame, (b) the response of the proposed frame (figures show the bandgap region zoomed in).

The following remarks can be observed from the above harmonic analysis results of the ordinary frame and the proposed frame:

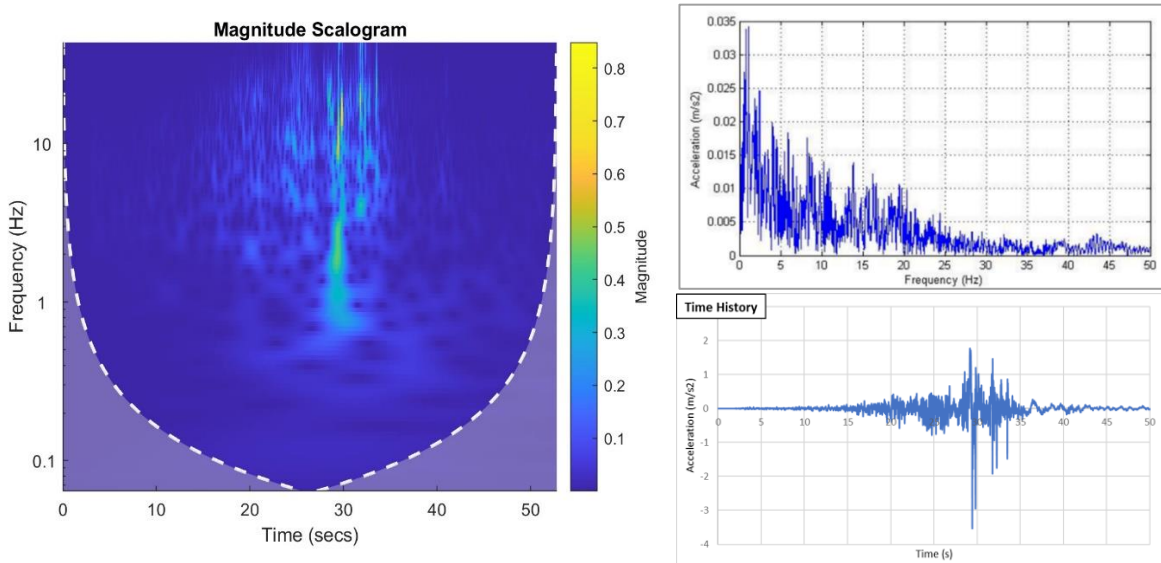
- In the ordinary frame, the dynamic magnification factor does not show any attenuation band, and the values are high in the shown frequency range.
- In the ordinary frame, the dynamic magnification factor,  $D$ , at the beam  $D_b$  and at the column  $D_c$  are almost identical, and this refers to the rigid connection between the beam and the column.
- In the proposed frame, the dynamic magnification factor shows a clear attenuation frequency band in the range from 5 Hz to 11.36 Hz, which exactly matches the designed frequency band gap calculated in section 3 with the method reported in [13].
- In the proposed frame, the dynamic magnification factor at the beam and the column are not identical. This is because of the existence of the proposed connection between the beam and the column, that is not rigid because of the existence of the spring (fig.1c). However, as shown in Fig.4, in the band gap frequency range, they both are closed to zero.

In the proposed frame, the dynamic magnification factor is nearly zero in the frequency band gap, which proves the success and validity of this research idea to introduce a frequency band gap.

### 4.3 Time-History Analysis Results and Discussion

A time history analysis was performed for both the proposed frame and the normal one. The response of the proposed frame under the loading of 9 different earthquakes is presented and compared with the response of a normal frame with the same dimensions and material properties. The frequency of the earthquakes ranging between 0.1 and 60 Hz was obtained using MATLAB software and both models were analysed under the loading of each earthquake (EQ.) using ANSYS software. The resulted top displacement and base shear of both models are presented below.

1- Chi-Chi (Taiwan) earthquake results: (Frequency range: 0.02-50.0 Hz)





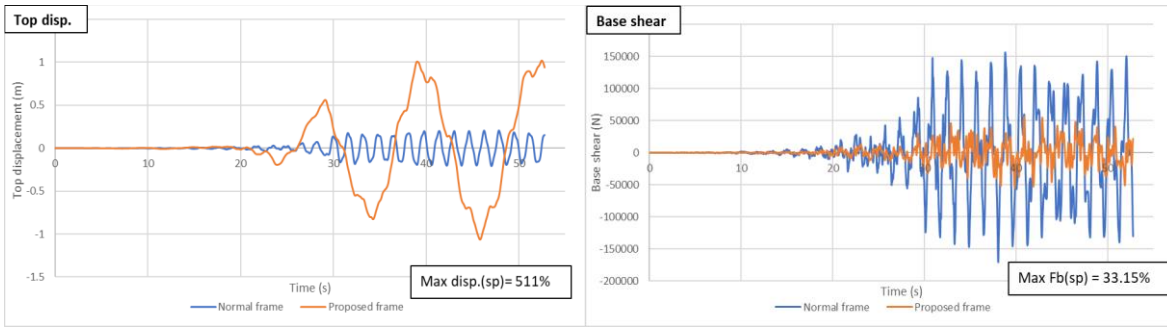


Fig. 5 Illustration of the frequency, time history and the magnitude scalogram for the Chi-Chi earthquake and the comparison between the resulted top displacement and the base shear for the normal frame and the new proposed frame.

As shown in the frequency chart of the earthquake Fig.5, the frequencies of the waves with the highest values of acceleration for this earthquake were outside the range of frequency bandgap calculated for the proposed frame. Through time-history analysis, the resulted maximum top displacement in the proposed frame was higher than that of the normal frame by a ratio of 511%. In contrast, the resulted maximum base shear in the proposed frame was less than that of the normal one by a ratio of 33.15%.

2- Friuli (Italy) earthquake results: (Frequency range: 0.1-30.0 Hz)

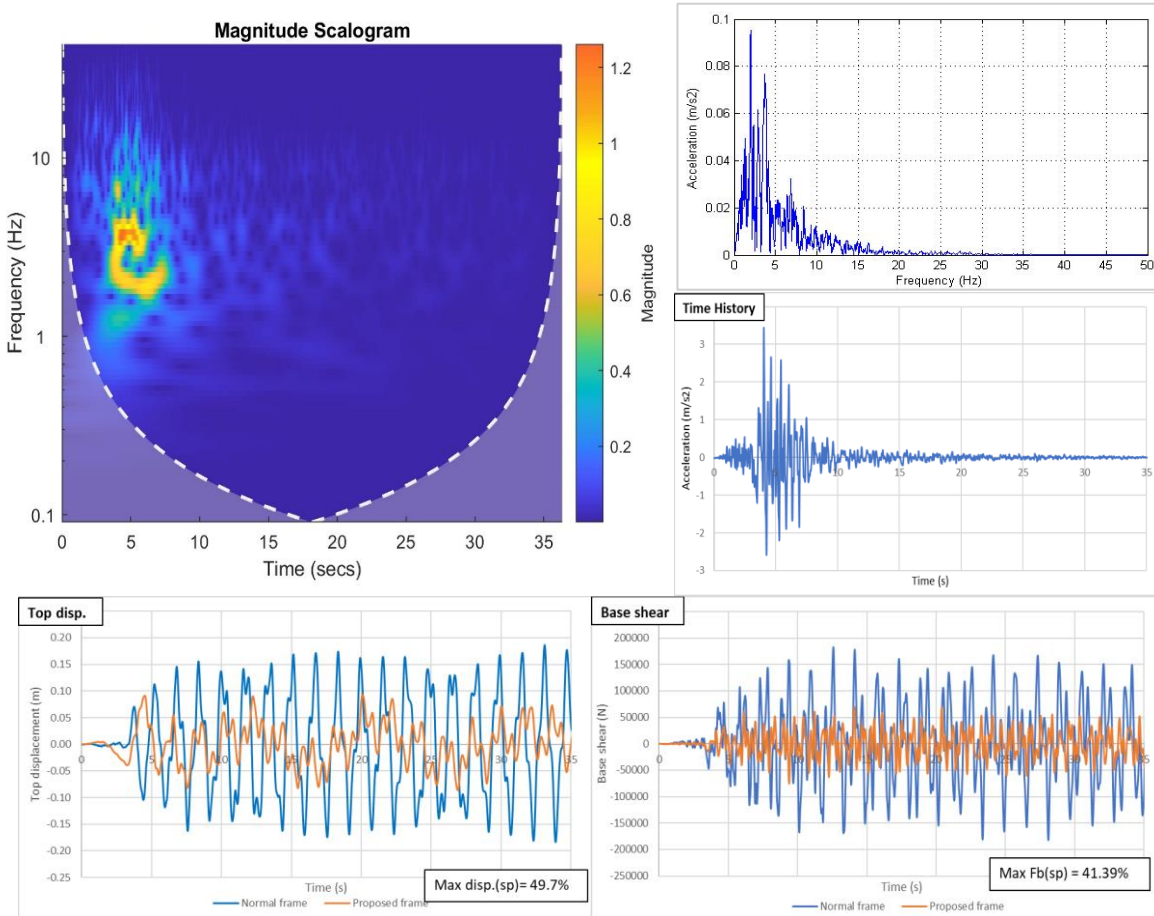


Fig. 6 Illustration of the frequency, time history and the magnitude scalogram for the Friuli earthquake and the comparison between the resulted top displacement and the base shear for the normal frame and the new proposed frame.

The value of the resulted maximum top displacement in the proposed frame was attenuated by a ratio of 49.7% of the value of the resulted top displacement in the normal one (see Fig.6). Also, the resulted maximum value of the base shear in the proposed frame was 41.39% of the resulted value of the base shear in the normal one.

3- Hollister (USA) earthquake results: (Frequency range: 0.11-11.0 Hz)

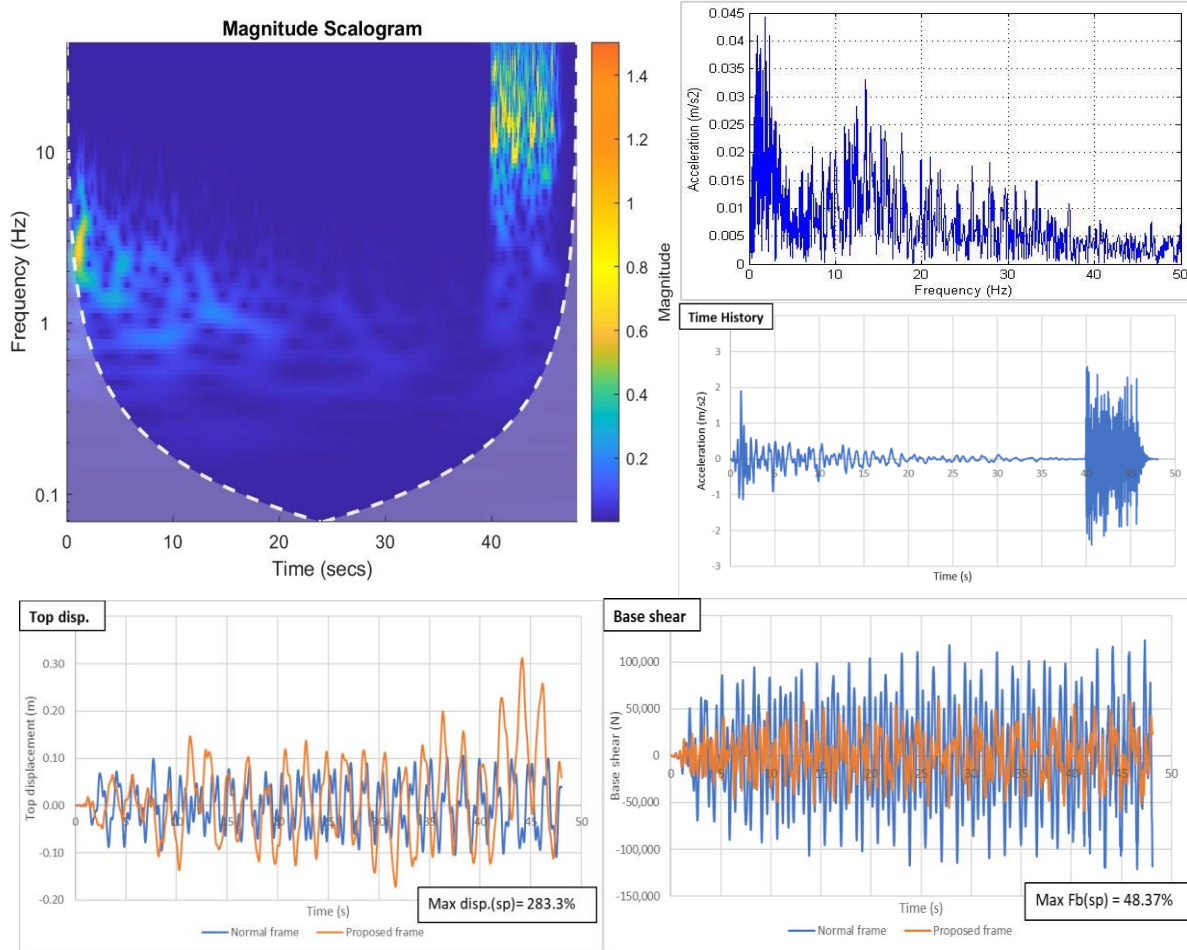
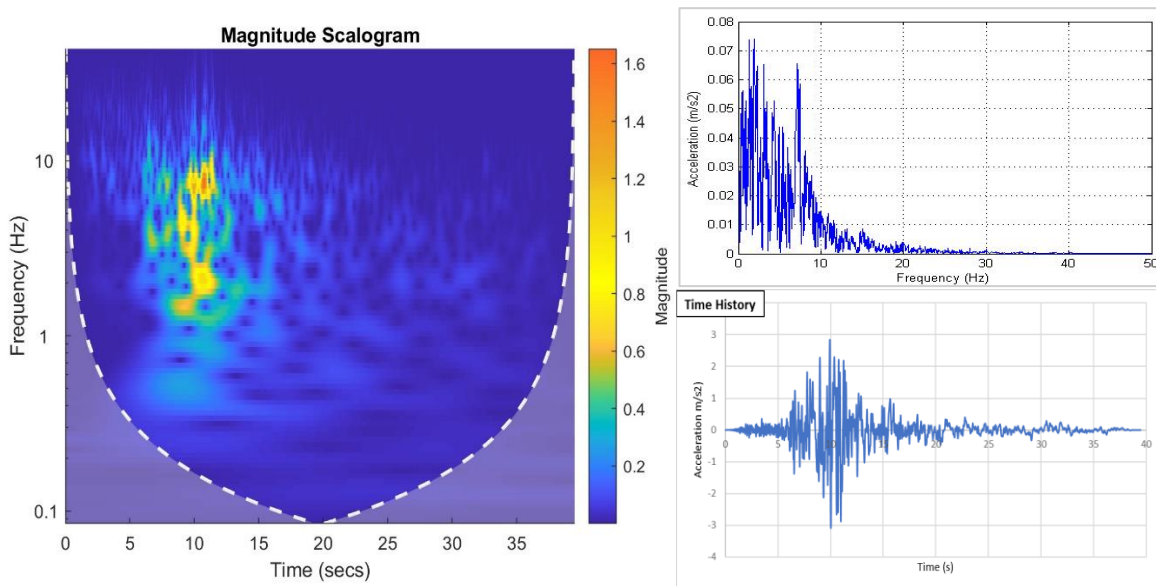


Fig. 7 Illustration of the frequency, time history and the magnitude scalogram for the Hollister earthquake and the comparison between the resulted top displacement and the base shear for the normal frame and the new proposed frame.

Through time-history analysis, under the loading of Hollister earthquake the values of the top displacement of both normal and proposed frame were close till the time was 40 sec. then the maximum top displacement in the proposed frame reached its maximum value which was 283.3% of that of the normal frame. In contrast, the resulted maximum base shear in the proposed frame was less than that of the normal one by a ratio of 48.37%. Most of the high acceleration values were outside the range of frequency bandgap that was calculated from 5 Hz to 11.36 Hz. As shown in Fig. 7 the highest values of accelerations are located from 0 to 5 Hz and from 10 Hz to 15 Hz.

4- The Imperial Valley (USA) earthquake results: (Frequency range: 0.1-40.0 Hz)



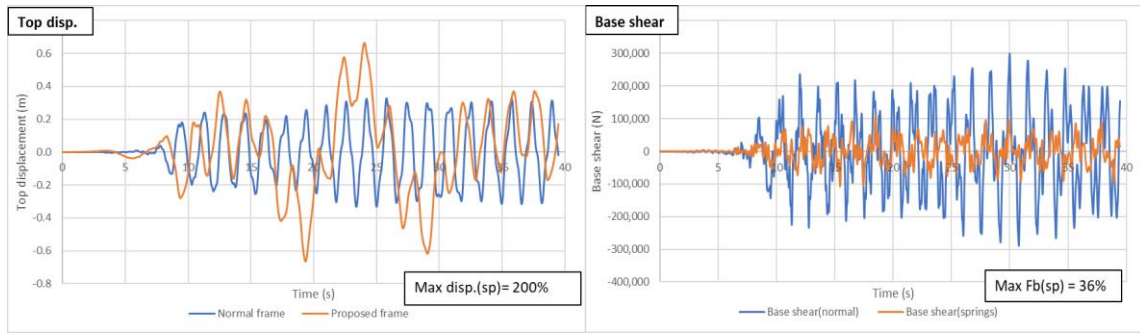


Fig. 8 Illustration of the frequency, time history and the magnitude scalogram for The Imperial Valley earthquake and the comparison between the resulted top displacement and the base shear for the normal frame and the new proposed frame.

Fig.8 shows the resulted maximum top displacement in the proposed frame was higher than that of the normal frame by a ratio of 200%. In contrast, the resulted maximum base shear in the proposed frame was less than that of the normal one by a ratio of 36%.

5- The Kocaeli (Turkey) earthquake results: (Frequency range: 0.07-50.0 Hz)

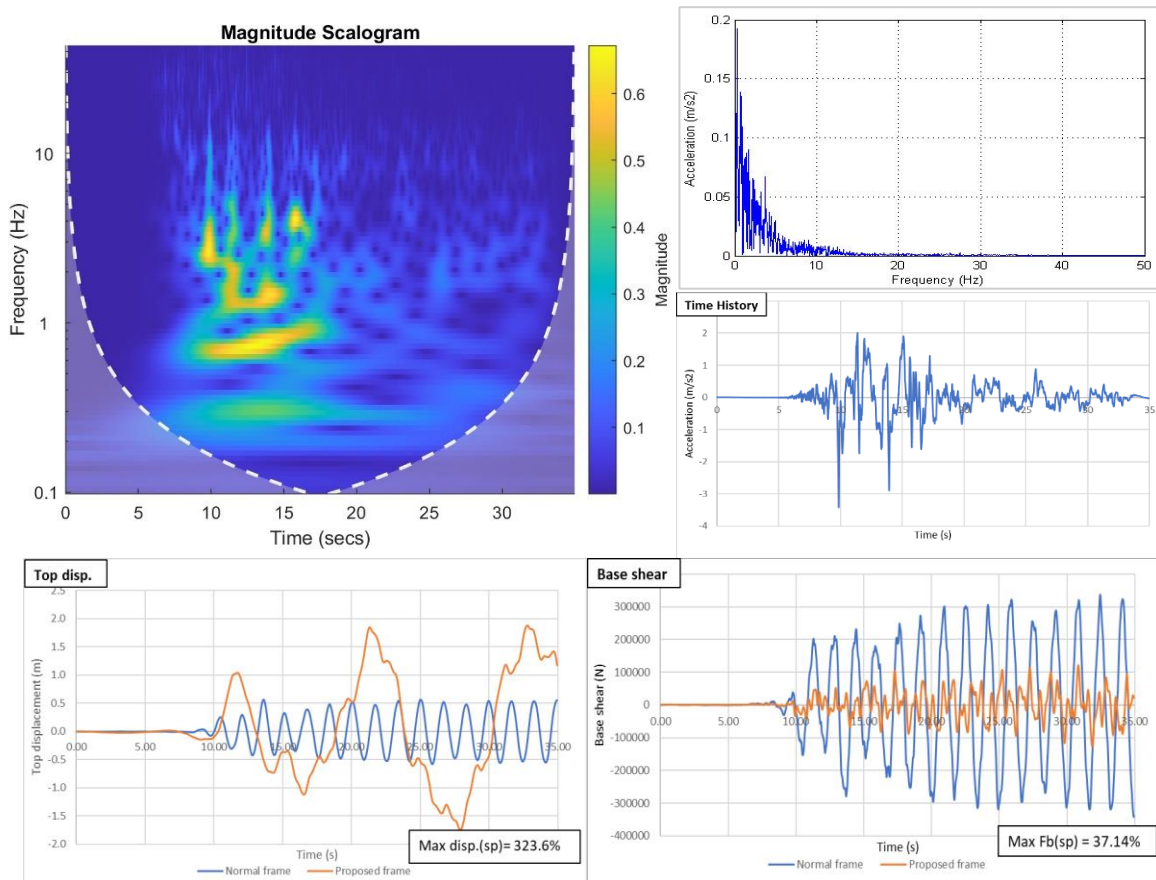


Fig. 9 Illustration of the frequency, time history and the magnitude scalogram for the Kocaeli earthquake and the comparison between the resulted top displacement and the base shear for the normal frame and the new proposed frame.

The majority of high intensity waves had frequencies ranging from 0 to 5 Hz as shown in the frequency chart Fig.9, and this resulted in a significantly high displacement in the proposed frame that reached 323.6% of the maximum displacement of the normal frame as presented in Fig.8. In contrast, the resulted maximum base shear in the proposed frame was less than that of the normal one by a ratio of 37.14%.

6- Landers (USA) earthquake results: (Frequency range: 0.08-60.0 Hz)

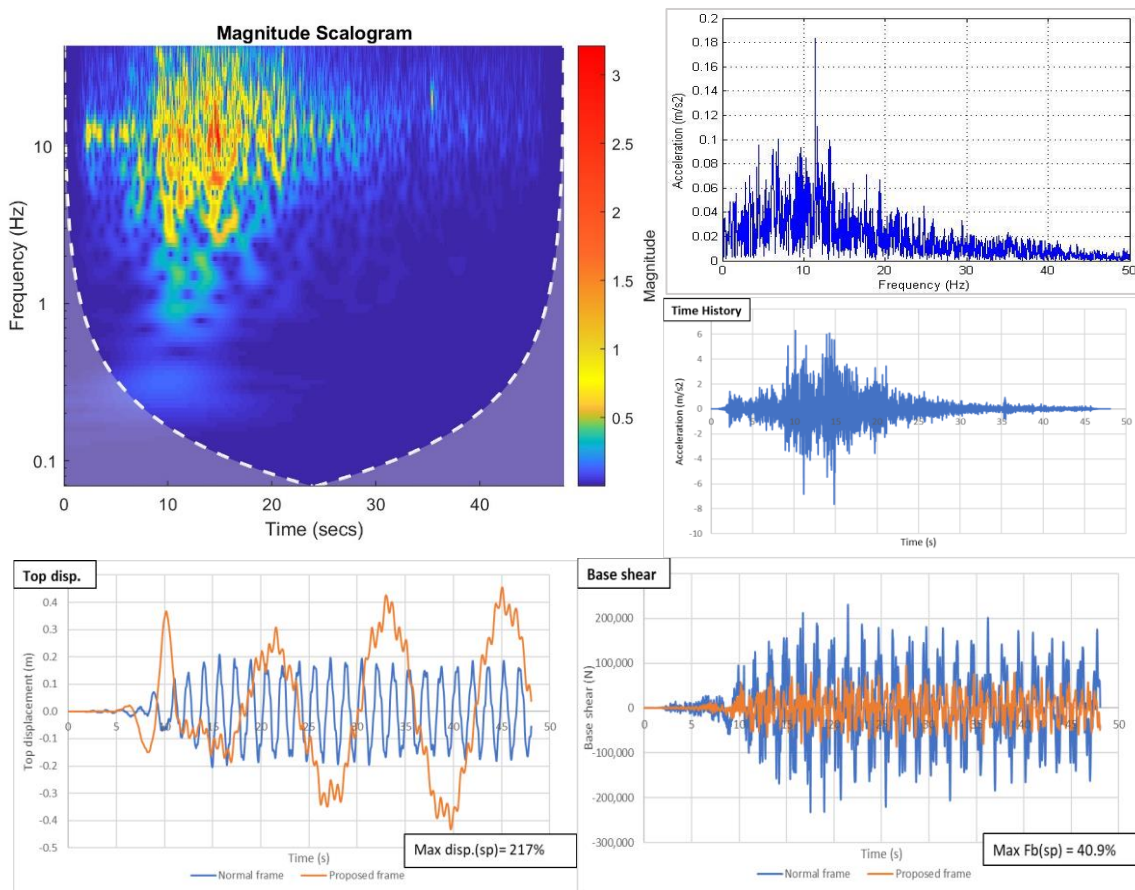
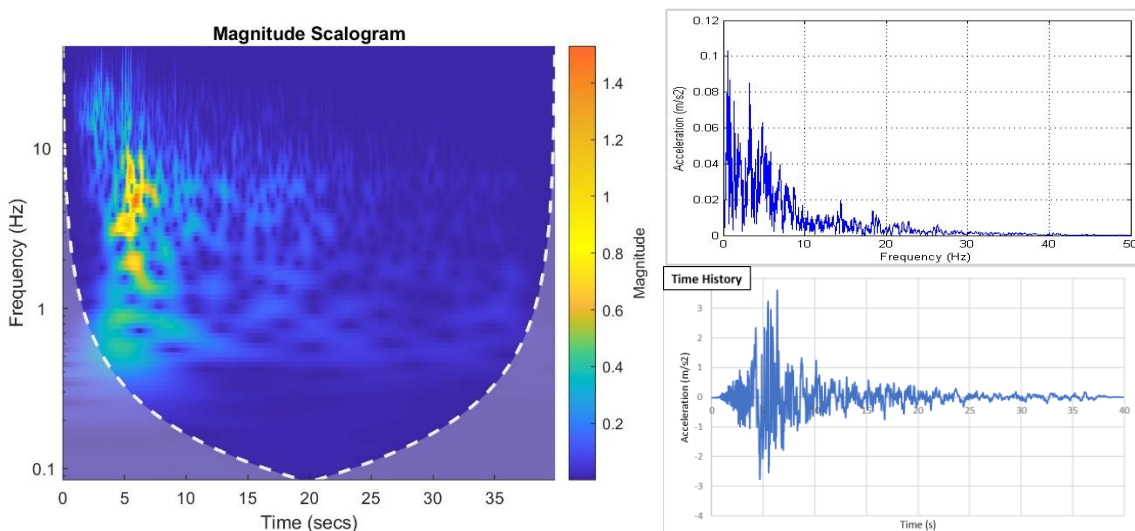


Fig. 10 Illustration of the frequency, time history and the magnitude scalogram for the Landers earthquake and the comparison between the resulted top displacement and the base shear for the normal frame and the new proposed frame.

The resulted maximum top displacement in the proposed frame was higher than that of the normal frame by a ratio of 217%. In contrast, the resulted maximum base shear in the proposed frame was less than that of the normal one by a ratio of 40.9%.

Although the Kocaeli earthquake is at the same frequency range as the Landers earthquake, the resulted displacement of the proposed frame under the influence of Kocaeli EQ. reached higher values than that of Landers EQ., because, in the Kocaeli frequency chart shown in Fig.9, most of the waves with high intensity had frequency values that are far from the frequency range of the attenuated region caused by the bandgap. However, in the Landers frequency chart shown in Fig.10, the high intensity waves were distributed inside and outside the range of frequency of the bandgap, which resulted in a significant reduction in the top displacement values.

7- The Loma Prieta (Turkey) earthquake results: (Frequency range: 0.1-40.0 Hz)



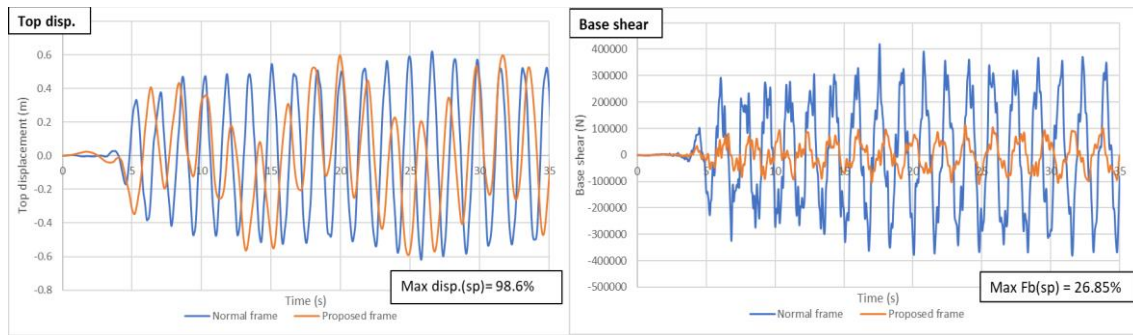


Fig. 11 Illustration of the frequency, time history and the magnitude scalogram for the Loma Prieta earthquake and the comparison between the resulted top displacement and the base shear for the normal frame and the new proposed frame.

Under the loading of the Loma Prieta EQ. shown in Fig.11, The value of the resulted maximum top displacement in the proposed frame was 98.6% of the value of the resulted top displacement in the normal one. A part of the high intensity waves was cancelled because the high intensity waves had frequencies close to the frequencies of the bandgap. Also, the resulted maximum value of the base shear in the proposed frame was 26.85% of the resulted value of the base shear in the normal one.

8- The Northridge (USA) earthquake results: (Frequency range: 0.12-23.0 Hz)

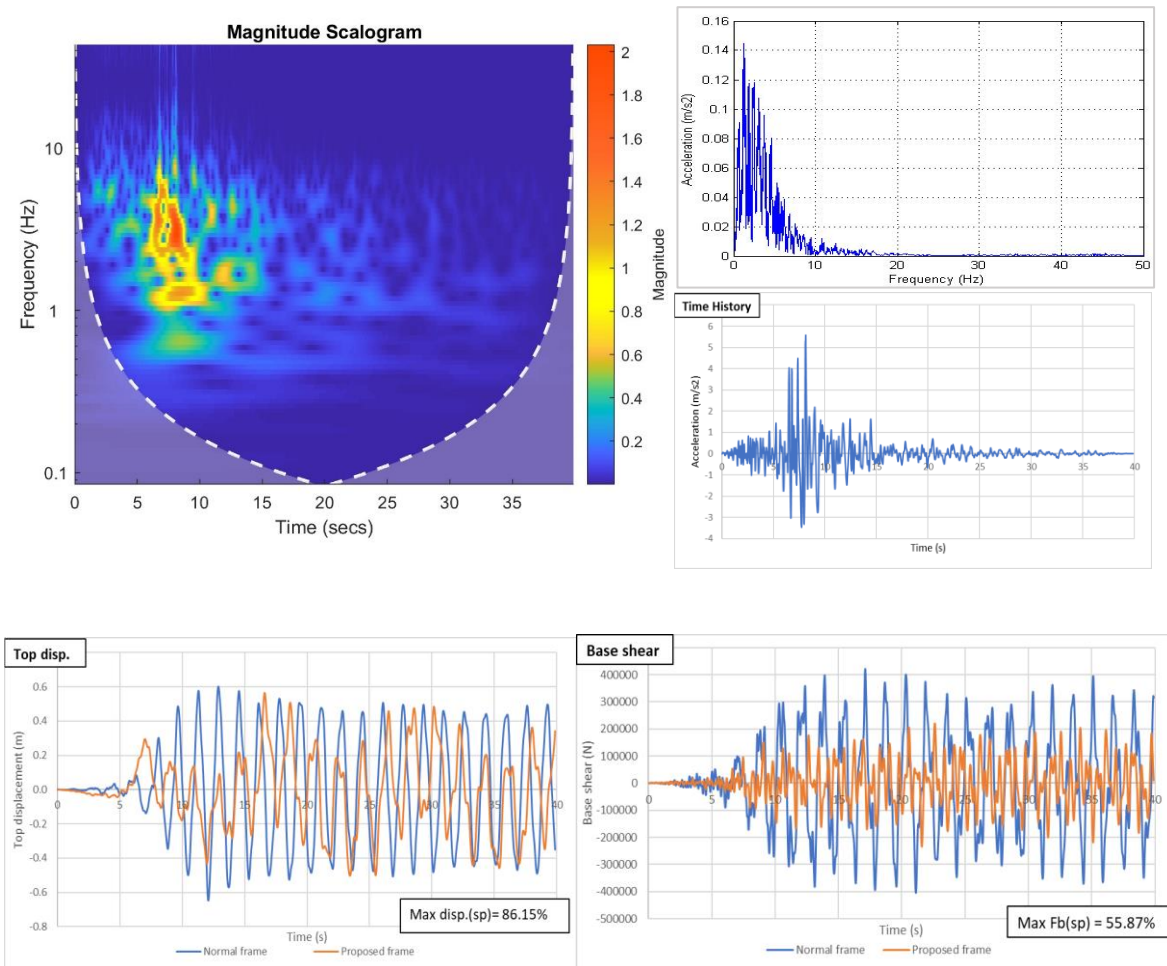


Fig. 12 Illustration of the frequency, time history and the magnitude scalogram for the Northridge earthquake and the comparison between the resulted top displacement and the base shear for the normal frame and the new proposed frame.

For the Northridge EQ. shown in Fig.12, the frequency range was lower than that of the Northridge EQ., Thus the value of the resulted maximum top displacement in the proposed frame was 86.15% of the value of the resulted top displacement in the normal one. Also, the resulted maximum value of the base shear in the proposed frame was 55.87% of the resulted value of the base shear in the normal one.

9- The Trinidad (USA) earthquake results: (Frequency range: 0.15-30.0 Hz)

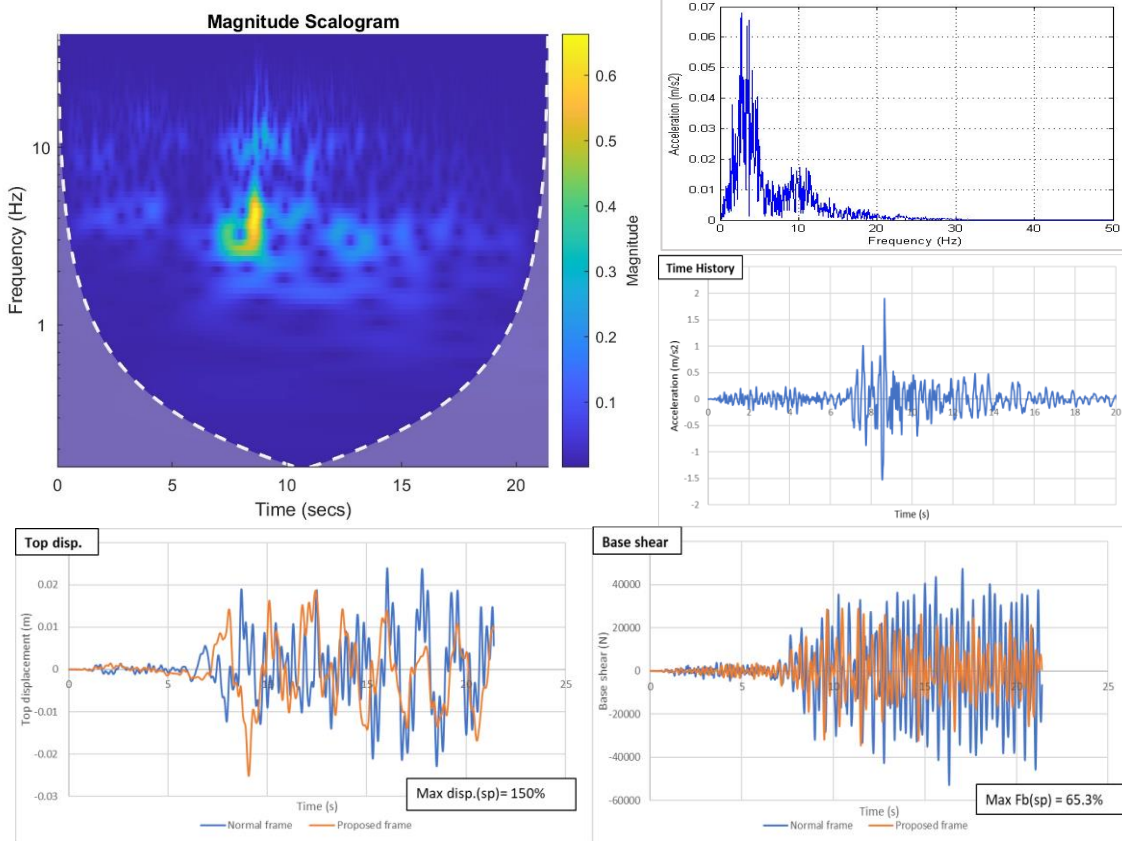


Fig. 13 Illustration of the frequency, time history and the magnitude scalogram for the Trinidad earthquake and the comparison between the resulted top displacement and the base shear for the normal frame and the new proposed frame.

The resulted maximum top displacement in the proposed frame and the normal one was almost the same under the loading of the Trinidad EQ. (shown in Fig.13) until it reached a peak value that was higher than that of the normal frame by a ratio of 150%. In contrast, the resulted maximum base shear in the proposed frame was less than that of the normal one by a ratio of 65.3%. The comparison between the maximum acceleration of the presented EQs, the resulted maximum top displacement and base shear for both proposed frame and normal frame as well as their ratios are shown in Table 4.

Table 4. the parameters measured and valued from the time-history analysis results.

EQ.	Maximum acceleration ( $a_g$ max) ( $m/s^2$ )	Maximum top displacement ( $\Delta_{max}$ ) (m)		$\frac{\Delta_{max 2}}{\Delta_{max 1}}$	Maximum Base shear ( $F_b$ max) (kN)		$\frac{F_b \text{ max } 2}{F_b \text{ max } 1}$
		Normal frame ( $\Delta_{max 1}$ )	Proposed frame ( $\Delta_{max 2}$ )		Normal frame ( $F_b \text{ max } 1$ )	Proposed frame ( $F_b \text{ max } 2$ )	
Chi-Chi (Taiwan)	3.53	0.208	1.06	511%	170	56.64	33.15%
Friuli (Italy)	3.44	0.187	0.093	49.7%	182.3	75.46	41.39%
Hollister (USA)	2.56	0.11	0.311	283.3%	123.38	59.68	48.37%
The Imperial Valley (USA)	3.08	0.33	0.66	200%	300.58	108.38	36%
The Kocaeli (Turkey)	3.42	0.58	1.87	323.6%	342.3	127.15	37.14%
Landers (USA)	7.64	0.209	0.454	217%	232.68	95.32	40.9%
The Loma Prieta (Turkey)	3.47	0.618	0.61	98.6%	420.7	112.99	26.85%
The Northridge (USA)	5.56	0.65	0.56	86.15%	420.5	234.96	55.87%
The Trinidad (USA)	1.89	0.02	0.03	150%	52.83	34.52	65.3%

In conclusion, only under the loading of the Friuli, Loma Prieta and Northridge earthquakes as shown in Fig.6, 11 and 12, the resulted maximum displacement of the proposed frame was less than the maximum displacement of the normal frame by an amount ranging from 1.4% to 50.3%. In contrast, the resulted maximum displacement of the proposed frame was higher than the maximum displacement of the normal frame by an amount ranging from 150% to 323.6% under the loading of the other earthquakes. For the earthquakes with the highest range of frequencies like Chichi and Kocaeli EQs, the resulted maximum top displacements were the highest as shown in Table 4, because the high intensity waves had frequencies far outside the range of the bandgap range, unlike Landers EQ. that had the waves with the highest intensity distributed close to the bandgap. Furthermore, the resulted base shear in the proposed frame was less than the resulted base shear in the normal frame under the loading of all 9 earthquakes by an amount ranging from 34.7% to 73.15%.

### 5. Expected dimensions of the new connection

In order to consider the dimensions of the new device and realising the new connection proposed, we studied the resulted difference in displacements of two points in several floors in the proposed frame. The first point is the one at the edge of the floor and the second is the one in the middle of the floor, see Fig.14. The difference between the 2 points was studied at the top of the frame, the sixth floor and the third floor.

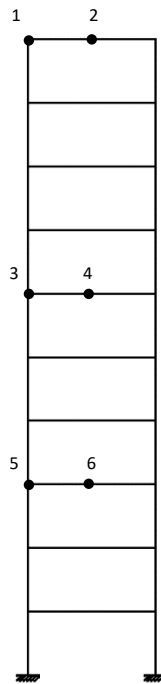


Fig. 14 The proposed frame: 1, 3 & 5 The points at the column of the frame in the steady-state response, 2, 4 & 6 The points at the middle of the beam in the steady-state response.

We studied the response of the frame under the loading of the Hollister earthquake for example. The differences between the resulted displacements at points 1 and 2 at the top floor, the sixth floor and the third floor are calculated and presented below in Fig.15.

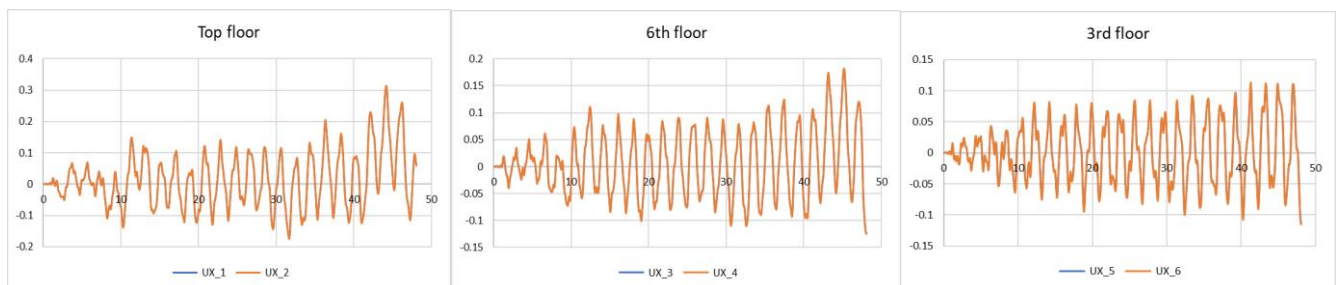


Fig. 15 the resulted displacements at the top floor, 6<sup>th</sup> floor, and 3<sup>rd</sup> floor.

The maximum difference between the resulted displacements at points 1 and 2 at the top floor was equal to 5.4 mm, while the maximum difference between the resulted displacements at points 3 and 4 at the sixth floor was equal to 4.5 mm and the maximum difference between the resulted displacements at points 5 and 6 was equal to 5.3 mm. Consequently, we can deduce the dimensions of the device that will represent the new connection in the proposed frame. In order to obtain the necessary

stiffness for the proposed connection, we can use the laminated rubber bearing discussed before in section 2. It can be considered as an economic and efficient seismic isolation technique.

## 6. Conclusion

The last decades, the concept of metamaterials has been investigated and its contribution in seismic protection of buildings has been proved either by installing metamaterial structures in the surrounding soil or above its surface or in the foundations of the building.

In this research, a new technique has been introduced where the metamaterial concept is applied in the building itself by converting the regular beam-column connection to a new proposed one. A new idea is introduced by implementing the metamaterial concept in the frame itself in order to create a frequency band gap when the frame is subjected to harmonic loadings. This idea can be achieved by converting the regular beam-column connection to a new proposed one, and this new connection has a spring connecting the beams with the frame column in each story, the stiffness of the spring can be adjusted and tailored with respect to the mass of the beams and columns in order to obtain a designated and desired frequency band gap, where no elastic waves can be transmitted or propagated through the structure. The proposed idea has been verified by performing modal analysis and harmonic analysis for the new proposed frame and the ordinary one. Moreover, the model was analysed under time history loading and its performance under 9 different earthquake loading was illustrated. Under the loading of 3 of the earthquake loadings, the resulted maximum displacement of the proposed frame was less than the maximum displacement of the normal frame by an amount ranging from 1.4% to 50.3% because the frequencies of the highest intensity waves were approaching or inside the frequency range of the calculated bandgap. Furthermore, we witnessed a reduction in the resulted base shear of the proposed frame under the loading of all 9 earthquakes by an amount ranging from 34.7% to 73.15%. That base shear reduction shows the enhancement of the lateral load handling capacity of the new system without any compromise in the structure weight.

A realisation of the new connection has been studied through calculating the difference in displacements between 2 points at different floors, one point at the edge of the floor and the other is at middle of the floor. The resulted difference in displacements ranged from 4.5 to 5.4 mm which offers us a great variety in choosing the device that can represent the new proposed connection. A real-life example for the proposed connection is presented but additional testing should be carried out to obtain a bearing that has the exact needed stiffness for the connection.

The results show the success and validity of the proposed idea where a frequency band gap has been created in the designated and calculated range.

This idea can be useful in many civil engineering applications in order to prevent harmful or undesirable elastic waves of vibrations. It can be used to design structural systems with tailored and tuned frequency band gap in the required range of frequencies to avoid or attenuate the harmful effects of undesirable elastic waves of seismic, wind or machine vibrations.

### Shortcomings and future work

The following are proposed for farther studies;

- For more realization of the current model, an experimental work can be investigated.
- A 3-D model simulation can be proposed to investigate the combined effect of metamaterials on the mitigation of vibrations in the structural system.
- The new proposed idea can be further applied and studied in the foundations of the structure or in the surrounding soil.

## 7. References

- [1] F. dell'Isola *et al.*, "Pantographic metamaterials: an example of mathematically driven design and of its technological challenges," *Continuum Mechanics and Thermodynamics*, vol. 31, no. 4, pp. 851–884, Jul. 2019, doi: 10.1007/s00161-018-0689-8.
- [2] G. Rosi, L. Placidi, and N. Auffray, "On the validity range of strain-gradient elasticity: A mixed static-dynamic identification procedure," *European Journal of Mechanics - A/Solids*, vol. 69, pp. 179–191, May 2018, doi: 10.1016/J.EUROMECHSOL.2017.12.005.
- [3] G. Rosi, L. Placidi, V. H. Nguyen, and S. Naili, "Wave propagation across a finite heterogeneous interphase modeled as an interface with material properties," *Mech Res Commun*, vol. 84, pp. 43–48, Sep. 2017, doi: 10.1016/J.MECHRESCOM.2017.06.004.



- [4] L. Placidi, G. Rosi, I. Giorgio, and A. Madeo, "Reflection and transmission of plane waves at surfaces carrying material properties and embedded in second gradient materials."
- [5] F. Dell'Isola, A. Madeo, and L. Placidi, "Linear plane wave propagation and normal transmission and reflection at discontinuity surfaces in second gradient 3D continua," *ZAMM Zeitschrift für Angewandte Mathematik und Mechanik*, vol. 92, no. 1, pp. 52–71, Jan. 2012, doi: 10.1002/zamm.201100022.
- [6] Y. Amer, A. El-Sayed, and E. Ahmed, "Vibration reduction of a non-linear ship model using positive position feedback controllers," *Int J Dyn Control*, vol. 10, Apr. 2022, doi: 10.1007/s40435-021-00801-8.
- [7] R. Desai, A. Guha, and P. Seshu, "Modelling and simulation of active and passive seat suspensions for vibration attenuation of vehicle occupants," *Int J Dyn Control*, vol. 9, no. 4, pp. 1423–1443, Dec. 2021, doi: 10.1007/s40435-021-00788-2.
- [8] X. Li *et al.*, "Optimization of vibration characteristics and directional propagation of plane waves in branching ligament structures of wind models," *Results Phys*, vol. 47, p. 106345, 2023, doi: <https://doi.org/10.1016/j.rinp.2023.106345>.
- [9] N. Nejadi Sadeghi, L. Placidi, M. Romeo, and A. Misra, "Frequency band gaps in dielectric granular metamaterials modulated by electric field," *Mech Res Commun*, vol. 95, pp. 96–103, Jan. 2019, doi: 10.1016/J.MECHRESCOM.2019.01.006.
- [10] X. Li *et al.*, "Bandgap tuning and in-plane wave propagation of chiral and anti-chiral hybrid metamaterials with assembled six oscillators," *Physica A: Statistical Mechanics and its Applications*, vol. 615, p. 128600, 2023, doi: <https://doi.org/10.1016/j.physa.2023.128600>.
- [11] X. Li *et al.*, "Integrated analysis of bandgap optimization regulation and wave propagation mechanism of hexagonal multi-ligament derived structures," *European Journal of Mechanics - A/Solids*, vol. 99, p. 104952, 2023, doi: <https://doi.org/10.1016/j.euromechsol.2023.104952>.
- [12] A. Madeo, P. Neff, I.-D. Ghiba, L. Placidi, and G. Rosi, "Wave propagation in relaxed micromorphic continua: modelling metamaterials with frequency band-gaps," Sep. 2013, doi: 10.1007/s00161-013-0329-2.
- [13] M. G. el Sherbiny and L. Placidi, "Discrete and continuous aspects of some metamaterial elastic structures with band gaps," *Archive of Applied Mechanics*, vol. 88, no. 10, pp. 1725–1742, Oct. 2018, doi: 10.1007/s00419-018-1399-1.
- [14] L. Placidi, M. G. el Sherbiny, and P. Baragatti, "EXPERIMENTAL INVESTIGATION FOR THE EXISTENCE OF FREQUENCY BAND GAP IN A MICROSTRUCTURE MODEL," *Mathematics and Mechanics of Complex Systems*, vol. 9, no. 4, pp. 413–421, 2021, doi: 10.2140/memocs.2021.9.413.
- [15] F. dell'Isola, I. Giorgio, and U. Andreaus, "Elastic pantographic 2D lattices: A numerical analysis on the static response and wave propagation," *Proceedings of the Estonian Academy of Sciences*, vol. 64, no. 3, pp. 219–225, Aug. 2015, doi: 10.3176/proc.2015.3.03.
- [16] S. Brûlé, E. H. Javelaud, S. Enoch, and S. Guenneau, "Experiments on seismic metamaterials: Molding surface waves," *Phys Rev Lett*, vol. 112, no. 13, Dec. 2013, doi: 10.1103/PhysRevLett.112.133901.
- [17] A. Colombi, D. Colquitt, P. Roux, S. Guenneau, and R. V. Craster, "A seismic metamaterial: The resonant metawedge," *Sci Rep*, vol. 6, Jun. 2016, doi: 10.1038/srep27717.
- [18] Q. Du, Y. Zeng, G. Huang, and H. Yang, "Elastic metamaterial-based seismic shield for both Lamb and surface waves," *AIP Adv*, vol. 7, no. 7, Jul. 2017, doi: 10.1063/1.4996716.
- [19] O. Casablanca *et al.*, "Seismic isolation of buildings using composite foundations based on metamaterials," *J Appl Phys*, vol. 123, no. 17, May 2018, doi: 10.1063/1.5018005.
- [20] A. Palermo, B. Yousefzadeh, C. Daraio, and A. Marzani, "Rayleigh wave propagation in nonlinear metasurfaces," Jul. 2021, doi: 10.1016/j.jsv.2021.116599.
- [21] D. K. Guo and T. Chen, "Seismic metamaterials for energy attenuation of shear horizontal waves in transversely isotropic media," *Mater Today Commun*, vol. 28, Sep. 2021, doi: 10.1016/j.mtcomm.2021.102526.
- [22] X. Wang, S. Wan, Y. Nian, P. Zhou, and Y. Zhu, "Periodic in-filled pipes embedded in semi-infinite space as seismic metamaterials for filtering ultra-low-frequency surface waves," *Constr Build Mater*, vol. 313, Dec. 2021, doi: 10.1016/j.conbuildmat.2021.125498.

- [23] X. Wu, Z. Wen, Y. Jin, T. Rabczuk, X. Zhuang, and B. Djafari-Rouhani, "Broadband Rayleigh wave attenuation by gradient metamaterials," *Int J Mech Sci*, vol. 205, Sep. 2021, doi: 10.1016/j.ijmecsci.2021.106592.
- [24] T. T. Huang *et al.*, "Based on auxetic foam: A novel type of seismic metamaterial for Lamb waves," *Eng Struct*, vol. 246, Nov. 2021, doi: 10.1016/j.engstruct.2021.112976.
- [25] T. V. Varma, B. Ungureanu, S. Sarkar, R. Craster, S. Guenneau, and S. Brûlé, "The Influence of Clamping, Structure Geometry, and Material on Seismic Metamaterial Performance," *Front Mater*, vol. 8, May 2021, doi: 10.3389/fmats.2021.603820.
- [26] X. Pu, Q. Meng, and Z. Shi, "Experimental studies on surface-wave isolation by periodic wave barriers," *Soil Dynamics and Earthquake Engineering*, vol. 130, Mar. 2020, doi: 10.1016/j.soildyn.2019.106000.
- [27] F. Sun, L. Xiao, and O. S. Bursi, "Quantification of seismic mitigation performance of periodic foundations with soil-structure interaction," *Soil Dynamics and Earthquake Engineering*, vol. 132, May 2020, doi: 10.1016/j.soildyn.2020.106089.
- [28] X. Liu, Y. Ren, and X. Song, "Combined attenuation zones of combined layered periodic foundations," *Applied Sciences (Switzerland)*, vol. 11, no. 15, Aug. 2021, doi: 10.3390/app11157114.
- [29] T. Li, Q. Su, and S. Kaewunruen, "Seismic metamaterial barriers for ground vibration mitigation in railways considering the train-track-soil dynamic interactions," *Constr Build Mater*, vol. 260, Nov. 2020, doi: 10.1016/j.conbuildmat.2020.119936.
- [30] X. Pu, A. Palermo, Z. Cheng, Z. Shi, and A. Marzani, "Seismic metasurfaces on porous layered media: Surface resonators and fluid-solid interaction effects on the propagation of Rayleigh waves," *Int J Eng Sci*, vol. 154, Sep. 2020, doi: 10.1016/j.ijengsci.2020.103347.
- [31] W. Liu, G. H. Yoon, B. Yi, Y. Yang, and Y. Chen, "Ultra-wide band gap metasurfaces for controlling seismic surface waves," *Extreme Mech Lett*, vol. 41, Nov. 2020, doi: 10.1016/j.eml.2020.101018.
- [32] A. Colombi, R. Zaccherini, G. Aguzzi, A. Palermo, and E. Chatzi, "Mitigation of seismic waves: Metabarriers and metafoundations bench tested," *J Sound Vib*, vol. 485, Oct. 2020, doi: 10.1016/j.jsv.2020.115537.
- [33] J. J. Marigo, K. Pham, A. Maurel, and S. Guenneau, "Effective model for elastic waves propagating in a substrate supporting a dense array of plates/beams with flexural resonances," *J Mech Phys Solids*, vol. 143, Oct. 2020, doi: 10.1016/j.jmps.2020.104029.
- [34] Muhammad, C. W. Lim, and J. N. Reddy, "Built-up structural steel sections as seismic metamaterials for surface wave attenuation with low frequency wide bandgap in layered soil medium," *Eng Struct*, vol. 188, pp. 440–451, Jun. 2019, doi: 10.1016/j.engstruct.2019.03.046.
- [35] M. Wang, F. fei Sun, J. qi Yang, and S. Nagarajaiah, "Seismic protection of SDOF systems with a negative stiffness amplifying damper," *Eng Struct*, vol. 190, pp. 128–141, Jul. 2019, doi: 10.1016/j.engstruct.2019.03.110.
- [36] M. Wang, F.-F. Sun, Y. Koetaka, L. Chen, S. Nagarajaiah, and X.-L. Du, "Frequency independent damped outrigger systems for multi-mode seismic control of super tall buildings with frequency independent negative stiffness enhancement," *Earthq Eng Struct Dyn*, vol. n/a, no. n/a, Apr. 2023, doi: <https://doi.org/10.1002/eqe.3891>.
- [37] L. Xiao, O. S. Bursi, M. Wang, S. Nagarajaiah, F. Sun, and X.-L. Du, "Metamaterial beams with negative stiffness absorbers and rotation: band-gap behavior and band-gap merging," *Eng Struct*, vol. 280, p. 115702, 2023, doi: <https://doi.org/10.1016/j.engstruct.2023.115702>.
- [38] B. Zhang, K. Wang, G. Lu, W. Qiu, and W. Yin, "Experimental and Seismic Response Study of Laminated Rubber Bearings Considering Different Friction Interfaces," *Buildings*, vol. 12, no. 10, Oct. 2022, doi: 10.3390/buildings12101526.